PAPER

[11C]-Methionine PET: dysembryoplastic neuroepithelial tumours compared with other epileptogenic brain neoplasms

D S Rosenberg, G Demarquay, A Jouvet, D Le Bars, N Streichenberger, M Sindou, N Kopp, F Mauguière, P Ryvlin

J Neurol Neurosurg Psychiatry 2005;**76**:1686–1692. doi: 10.1136/jnnp.2004.051607

See end of article for authors' affiliations

Correspondence to: Professor Ryvlin, Cermep, Hopital Neurologique, 59 Bd Pinel, Lyon, 69003, France; ryvlin@cermep.fr

Received 10 August 2004
Revised version received 29 April 2005
Accepted 2 May 2005

Background and objectives: Brain tumours responsible for longstanding partial epilepsy are characterised by a high prevalence of dysembryoplastic neuroepithelial tumour (DNT), whose natural evolution is much more benign than that of gliomas. The preoperative diagnosis of DNT, which is not yet feasible on the basis of available clinical and imaging data, would help optimise the therapeutic strategy for this type of tumour. This study tested whether [11C]-methionine positron emission tomography (MET-PET) could help to distinguish DNTs from other epileptogenic brain tumours.
Methods: Prospective study of 27 patients with partial epilepsy of at least six months duration related to a non-rapidly progressing brain tumour on magnetic resonance imaging (MRI). A structured visual analysis, which distinguished between normal, moderately abnormal, or markedly abnormal tumour methionine uptake, as well as various regions of interest and semiquantitative measurements were conducted.
Results: Pathological results showed 11 DNTs (41%), 5 gangliogliomas (18%), and 11 gliomas (41%). MET-PET visual findings significantly differed between the various tumour types ($p<0.0002$), regardless of gadolinium enhancement on MRI, and were confirmed by semiquantitative analysis ($p<0.001$ for all calculated ratios). All gliomas and gangliogliomas were associated with moderately or markedly increased tumour methionine uptake, whereas 7/11 DNTs had a normal methionine uptake, including all six located in the mesiotemporal structures. No DNT presented with a marked MET-PET abnormality.
Conclusion: Normal MET-PET findings in patient with an epileptogenic and non-rapidly progressing brain tumour are suggestive of DNT, whereas a markedly increased tumour methionine uptake makes this diagnosis unlikely.

A brain tumour is found in 30–55% of patients with surgically treated, drug resistant partial epilepsy.[1–4] Epileptogenic tumours, responsible for such epilepsies, are strikingly different from conventional cerebral neoplasms, in terms of both prognosis and neuropathological findings.[5 6]

Dysembryoplastic neuroepithelial tumours (DNTs) and gangliogliomas, which appear to account for most of these tumours, remain difficult to identify,[7–9] and several authors have acknowledged the possibility of misdiagnosing DNTs and gangliogliomas as oligoastrocytoma, oligodendroglioma, and astrocytoma.[3 4 7–11] Such misclassifications may lead to unnecessary and potentially dangerous treatments.[12 13] Indeed, unlike most other forms of brain tumours, DNTs are supposed to be non-progressive and not life threatening tumours, with a single published case of suspected malignant transformation.[14] Although magnetic resonance imaging (MRI) provides some hints about the pathology underlying epileptogenic brain tumours, it is not reliable enough to assure the diagnosis of DNT.[15] Thus other methods have been advocated for the differential diagnosis of these tumours.

Positron emission tomography (PET) has been widely used in an attempt to grade brain tumours. [18F]-fluorodeoxyglucose (FDG) as well as [11C]-methionine (MET) can distinguish high grade gliomas from low grade gliomas,[16–21] with more important increased methionine uptake in the World Health Organization (WHO) grades III and IV than in grades I and II gliomas.[22–34] Only small series have been published on FDG and MET-PET findings in glioneuronal tumours.[35–39]

In this study of 27 patients with epileptogenic brain tumours, we tested the ability of MET-PET to help distinguish DNTs from gangliogliomas and others gliomas.

PATIENTS AND METHODS

Patients

From 1995 to 2002 we prospectively selected all patients who had been consecutively referred to our epilepsy department for partial epilepsy associated with an MRI abnormality suggesting a non-rapidly progressing brain tumour. All patients gave informed consent to participate in the study, and the local ethic committee approved the study, which conformed to the Declaration of Helsinki. We excluded those patients whose tumour had been symptomatic for less than six months or was associated with the following clinical or MRI signs, indicating a rapid tumour growth:

- a significant progressive neurological deterioration other than changes in seizure frequency and severity
- a clear-cut mass effect with midline displacement on neuroimaging data
- a significant increase in the tumour size on two consecutive MRI.

From the 30 patients who entered this PET study, we selected all those who had been operated on, and where the

Abbreviations: DNT, dysembryoplastic neuroepithelial tumour; T/C, tumour-to-contralateral homotopic ratio; MET-PET, [11C]-methionine positron emission tomography; MRI, magnetic resonance imaging; OR, tumour-to-contralateral occipital ratio; ROI, region of interest

quality of MET-PET and pathological data was considered sufficiently high to allow reliable analysis and correlations. Overall, 27 patients met the above criteria and are included in this report.

MRI

We used a 1.5 T device (Magnetom 63SP; Siemens, Erlangen, Germany) and included an axial or coronal spin echo T1 sequence (TR: 600 ms, TE: 12 ms) with and without gadolinium injection, and an axial spin echo T2 sequence (TR: 3000 ms, TE: 16 ms and 98 ms) perpendicular to the T1 sequence. In 20 patients only, a 3D T1 acquisition sequence (TR: 9.7 ms, TE: 4 ms) was performed.

PET

Data acquisition

We used two different cameras for the MET-PET scanning. The first 11 patients were scanned after receiving an intravenous bolus injection of 440 MBq of [^{11}C]-methionine with an LETI TTV03 (Grenoble, France) camera, providing seven 9 mm thick slices with an in-plane resolution of 7 mm full width at half maximum (FWHM). Data were acquired in two dimensional mode, planes oriented parallel to the orbitomeatal line. The others 16 patients received an intravenous bolus injection of 18.5 + 2.6 MBq/kg of [^{11}C]-methionine, and they underwent scanning using a high resolution tomograph (HR+ Siemens, Erlangen, Germany). Three dimensional data were acquired, providing 63 slices, 2.4 mm thick, with an isotropic spatial resolution of 5 mm FWHM. Before injection, we carried out transmission scanning for attenuation correction using three ^{68}Ge rod sources. For both cameras, static emission scanning was performed during a 20 minute period, beginning 35 minutes after the [^{11}C]-methionine injection, as has been done in several other studies.[31 33 34 36] Images were corrected for scatter and attenuation, and reconstructed using a filtered back projection.

PET

Data analysis

Visual analysis

Two of the investigators (DR, PR) independently performed a visual analysis of PET data, blinded to all other clinical and MRI data except the anatomical location of the tumour. We first determined whether the degree of methionine uptake within the tumour was significantly increased when compared with the surrounding brain and the contralateral homotopic region. If an increase was observed, we distinguished various degrees of abnormal methionine uptake using the contralateral occipital cortex as a reference. We used the contralateral occipital cortex as a reference because, in our experience, this brain region has consistently proved to display the highest methionine uptake among the entire non-tumoral cortical regions. The result of the visual analysis was classified based on the following definitions:

- Normal tumour methionine uptake—no visually detectable difference between the tumour and the surrounding or contralateral homotopic brain regions
- Moderately increased tumour methionine uptake—the tumour uptake clearly exceeds the uptake in surrounding cortical areas and in the contralateral homotopic region, but remains lower or comparable to that of the contralateral occipital cortex
- Markedly increased tumour methionine uptake—the tumour uptake clearly exceeds that observed in the contralateral occipital cortex

Semiquantitative analysis

We performed a semiquantitative analysis, using two sets of regions of interest (ROIs). The placement of the first set of ROIs required coregistered MRI and PET data, which were only available for the 20 patients who benefited from a 3D MRI. We manually traced irregular ROIs along the visually detected tumour borders on each MRI slice displaying the tumour, excluding areas of clear-cut necrosis or cyst. A flipped copy of each of these ROIs was placed over the contralateral homotopic region and readjusted to precisely match the outer border of the cortical ribbon. After coregistration with MRI, we transferred the tumoral (T) as well as the contralateral homotopic ROIs (C) onto the PET images and measured the mean regional count of radioactivity within these ROIs. We then calculated the mean tumour-to-contralateral homotopic ratio (mean T/C = T/C). The second set of ROIs corresponded to circular regions, 5 mm in diameter, which were directly placed onto the PET images. These ROIs were placed over the portion of the tumour displaying the highest [^{11}C]-methionine uptake (Tc = tumour circular ROI), the contralateral homotopic cortical region (Cc = contralateral circular ROI), and the most active area within the contralateral occipital cortex (Oc = occipital circular ROI), on a single slice each. This procedure was undertaken in all patients showing a visually detectable increased tumour methionine uptake, including those who did not benefit from coregistration of MRI and PET images (n = 5). It was also undertaken in the subset of patients with no visually detectable increased tumour methionine uptake, by placing the circular ROI over the most active voxels within the tumour border as delineated by coregistered MRI and PET data (n = 5). Only 2/27 patients (patient 4 and 7), whose MET-PET showed normal findings and who did not benefit from a 3D T1 MRI, were not included in this analysis. In the remaining 25 patients, we calculated two ratios:

- Maximal tumour-to-contralateral homotopic ratio (Max T/C) = Tc/Cc
- Maximal tumour-to-contralateral occipital ratio (OR) = Tc/Oc

Surgical procedure

A total of 24 patients (89%) benefited from a total (n = 18; 67%) or subtotal (n = 6; 22%) removal of their tumour. The remaining three patients (11%) underwent a biopsy, and the size and quality of the specimen enabled a conclusive pathological diagnosis.

Pathological analysis and diagnosis

Sections of formalin-fixed tissues were processed for histological staining using either the haemalum–phloxine safranin or the haematoxylin–eosin technique. Immunohistochemical stains, applied on routinely fixed and paraffin-embedded sections, were prepared for selected cases, using the avidin–biotin complex method and the following antisera: anti-GFAP (glial fibrillary acidic protein), anti-NF (neurofilament protein), anti-NSE (neurone specific enolase), antisynaptophysin, antivimentin, anti-S100 protein, and anti-Leu-7. These specimens were analysed at our institution by neuropathologists trained in the evaluation of epileptogenic low grade tumours, and ultimately classified according to the WHO classification. However, where the diagnosis remained uncertain, the specimens were sent to two other pathologists renowned for their experience in epileptogenic brain tumours (C Daumas-Duport, Saint-Anne Hospital, Paris, and B Pasquier, Albert Michallon Hospital, Grenoble, France) for further evaluation, which led to a consensual conclusion in all cases.

Table 1 Individual pathological, clinical, MRI, and PET-MET data

	Clinical data				MRI data				PET-MET data					
Patient no	Sex	Age	Age at epilepsy onset (years)	Epilepsy duration (years)	Location	Side	Gadolinium enhancement	Tumour size (best diameter) in mm	Visual methionine uptake	Mean T/C	Max T/C	OR	Camera	Pathological data
1	M	24	21	3	It	R	+	26	Normal	0.95	1.15	0.94	TTV	DNT
2	F	24	19	5	It	R	+	32	Marked	1.95	2.7	1.89	TTV	Pleomorphic Xanthoastrocytoma II
3	M	32	25	7	I + Fr + P	R	+	54	Marked	NA	5.8	2.7	TTV	Oligodendroglioma III
4	F	18	13	5	mT	L	+	20	Normal	NA	NA	NA	TTV	DNT
5	M	31	14	17	mT	L	–	13	Normal	0.63	0.66	0.44	TTV	DNT
6	F	46	34	12	Fr + T	R	–	53	Marked	NA	3.63	1.86	TTV	Oligodendroglioma III
7	M	22	10	12	mT	R	–	30	Normal	NA	NA	NA	TTV	DNT
8	M	56	50	6	O + It	L	–	62	Marked	1.53	2.93	1.62	TTV	Oligodendroglioma III
9	F	13	10	3	mT	R	+	28	Moderate	1.25	1.76	0.85	TTV	Ganglioglioma
10	M	23	3	20	O	L	NA	35	Marked	NA	2.25	1.14	TTV	Ganglioglioma
11	M	19	17	2.5	Fr	L + R	+	33	Marked	1.78	1.9	1.83	TTV	Pilocytic Astrocytoma I
12	M	12	10	2	mT	R	+	22	Moderate	1.74	2.2	1.1	HR+	Ganglioglioma
13	F	42	37	5	mT	L	–	25	Normal	1.04	1.3	0.88	HR+	DNT
14	F	10	7	3	O + It	L	–	35	Moderate	0.91	1.7	1.05	HR+	DNT
15	F	16	2	14	mT	R	+	19	Moderate	2.04	2.33	1.35	HR+	Ganglioglioma
16	F	44	1	43	O + It	R	–	28	Moderate	1.30	1.76	1.16	HR+	Ganglioglioma
17	F	8	1	7	T + Fr	L	–	62	Moderate	NA	1.64	0.85	HR+	Oligodendroglioma II
18	M	40	25	15	Fr	R	–	51	Marked	1.70	3.37	2.35	HR+	Oligodendroglioma II
19	F	46	30	6	P	L	–	43	Moderate	1.22	1.7	1.07	HR+	DNT
20	M	32	18	14	mT	L	–	31	Normal	1.17	1.07	0.81	HR+	DNT
21	F	27	25	1.5	It	L	NA	27	Moderate	NA	1.88	1.19	HR+	DNT
22	M	43	42	1.5	mT	R	–	32	Marked	1.42	3.11	1.9	HR+	Astrocytoma III
23	M	26	26	8 months	I + Fr + T	R	–	69	Moderate	1.28	2.9	1.31	HR+	Oligoastrocytoma II
24	F	18	8	10	It + mT	L	–	29	Moderate	1.06	1.7	1.2	HR+	DNT
25	M	42	33	9	Fr	R	–	38	Moderate	1.66	2.01	1.23	HR+	Oligoastrocytoma II
26	M	27	18	9	mT	L	+	22	Normal	1.24	1.19	0.65	HR+	DNT
27	M	41	35	6	O + It	L	+	48	Marked	2.27	3.37	2.32	HR+	Oligodendroglioma II

DNT, dysembryoplastic neuroepithelial tumour; F, female; Fr, frontal; I, insula; L, left; Lt, lateral temporal; M, male; max T/C, maximal tumour-to-contralateral homotopic ratio; mean T/C, mean tumor-to-contralateral homotopic ratio; MET-PET, [^{11}C]-methionine positron emission tomography; mT, mesial temporal; MRI, magnetic resonance imaging; NA, not available; O, occipital; OR, tumour-to-contralateral occipital ratio; P, parietal; R, right.

Statistical analysis

For visual analysis, three types of tumour were considered: DNTs, gangliogliomas, and gliomas (including astrocytomas, oligodendrogliomas, and oligoastrocytomas of various grades). We looked for correlations between the tumour type, its anatomical location, as well as the presence of contrast enhancement on MRI and that of a visually detectable increased tumour methionine uptake on MET-PET images, using the χ^2 statistic. For the semiquantitative MET-PET analysis we used a one factor analysis of variance and further separated the gliomas in low and high grade tumours, thus considering four groups: DNTs, gangliogliomas, low grade gliomas, and high grade gliomas.

RESULTS

Clinical and pathological data

Clinical and pathological data of the participating patients (15 men, 12 women; mean (SD) age at epilepsy onset 20 (13) years; mean (SD) duration of epilepsy 8.5 (8.2) years, range 8 months to 43 years) are presented in table 1. Seizures were not fully controlled by antiepileptic drugs in 83% of patients. None of the patients had a neurological deficit at the time of the PET study. The 27 tumours included 11 DNTs, 5 gangliogliomas, and 11 gliomas (1 pilocytic astrocytoma, 1 pleomorphic xanthoastrocytoma, 1 astrocytoma grade III, 6 oligodendrogliomas (3 grade II and 3 grade III), and 2 oligoastrocytomas grade II).

MRI findings

Fourteen tumours (52%) were located in the temporal lobe, including 11 within the mesial temporal structures. The rest of the tumours were found in the frontal (n = 7, 26%), the occipital (n = 5, 18%), or the parietal (n = 1, 4%) lobe. Glioneuronal tumours were more frequently located in mesial temporal structures (63%; including 64% of DNTs and 60% of gangliogliomas) than gliomas (10%) ($p<0.05$).

MET-PET findings (see table 1)

Visual analysis demonstrated an increased methionine uptake within the tumour in 20 patients (74%), which was classified as moderate in 11 (55%), and marked in 9 (45%). No increased uptake was detected in seven patients (26%) (fig 1). There was no correlation between the presence of increased methionine uptake and gadolinium enhancement on MRI, the former being observed in 73% of gadolinium enhanced tumours and in 71% of those without gadolinium enhancement (table 2).

MET-PET visual findings correlated with the pathological data ($p<0.0002$) (table 3). In fact, the lack of increased methionine uptake was only observed in DNTs, 7/11 demonstrating that pattern. The difference between DNTs and the other types of tumour was even more pronounced in the subset of mesial temporal lesions, where all DNTs displayed normal findings on MET-PET (n = 6), whereas all the other tumours (n = 4 (3 gangliogliomas, 1 astrocytoma)) demonstrated an increased methionine uptake. Thus, in our study population, normal MET-PET findings were only associated with DNTs, whereas the presence of a marked increase in methionine uptake was not observed in glioneuronal tumours with the exception of one ganglioglioma. Moderate increase in methionine uptake was associated with all types of tumour except mesiotemporal DNTs.

The semiquantitative analysis also demonstrated significant differences between the four types of tumour for the three calculated ratios (table 4): mean T/C ($p<0.001$), max T/C ($p<0.0001$), and OR ($p<0.0001$). Post hoc tests showed that DNTs were associated with lower ratios than gangliogliomas (mean T/C: $p<0.005$) as well as low grade (mean T/C: $p<0.0001$; max T/C: $p<0.003$; OR: $p<0.001$) and high grade gliomas (max T/C: $p<0.0001$; OR: $p<0.0001$). Furthermore, gangliogliomas were associated with lower ratios than low grade (OR: $p<0.05$) and high grade (max T/C:

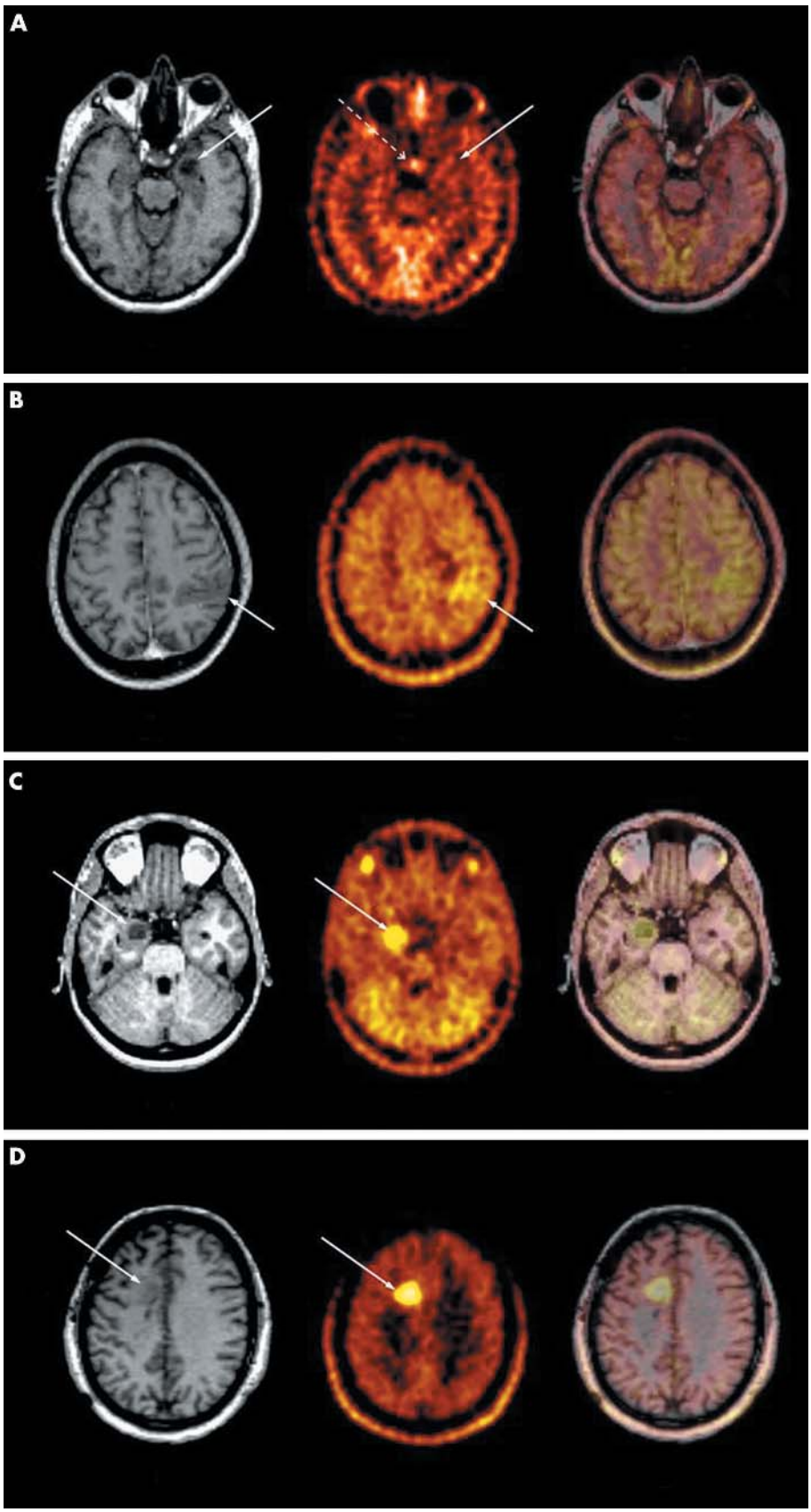

Figure 1 Examples of T1-weighted magnetic resonance images (left panel), methionine (MET) uptake (middle panel) and coregistered magnetic resonance imaging (MRI) and positron emission tomography (PET) data (right panel) for the three major tumour types. Arrows indicate tumour location on MRI and the corresponding methionine uptake on PET images. (A) Left mesial temporal dysembryoplastic neuroepithelial tumour (DNT), which was not associated with a visually detectable increased methionine uptake on raw MET-PET image, as well as on the coregistered MRI and PET data (patient no 13). The dotted arrow points to the hypophyseal region, which is physiologically associated with a higher methionine uptake than other neighbouring cerebral structures. (B) Left neocortical (parietal) DNT observed on T1-weighted MRI with a moderately increased methionine uptake on raw MET-PET image and coregistered MRI-PET data (patient no 19). (C) Right mesial temporal ganglioglioma associated with a moderately increased methionine uptake (patient no 15). (D) Right frontal glioma (oligodendroglioma grade II) corresponding to a hypodense area without gadolinium enhancement on T1-weighted MRI but associated with a markedly increased methionine uptake (patient no 18).

Table 2 Lack of association* between gadolinium (Gd) enhancement on magnetic resonance imaging (MRI) and qualitative [^{11}C]-methionine positron emission tomography findings

Visual MET-PET findings	With Gd enhancement	Without Gd enhancement
Normal	3	4
Moderate	3	7
Marked	4	4

*p = non-significant.

p<0.001; OR: p<0.003) gliomas. As already reported by others,[28–40] we also found an increased methionine uptake in gliomas, more pronounced in high grade than low grade tumours for max T/C and OR.

Results of the semiquantitative data analysis also significantly differed between the three types of visual MET-PET findings (mean T/C: p<0.004; max T/C: p<0.0001; OR: p<0.0001), with the lowest values associated with normal MET-PET findings and the highest with marked abnormalities. Although individual ratios values partly overlapped between the groups (see table 1), there was a cut-off for the max T/C between tumours with normal methionine uptake (⩽1.3) and those with moderate or marked methionine uptake (⩾1.64).

DISCUSSION

In this largest MET-PET series of patients with non-rapidly progressing epileptogenic brain tumours, we have shown that DNT, which is distinct from other low-grade tumours from a prognostic and therapeutic point of view, proved to be associated with a specific MET-PET finding—that is, normal methionine uptake in 7/11 cases, and in all those located in the mesial temporal region. Conversely, all other types of epileptogenic brain tumour displayed an increased methionine uptake in our study population. These results suggest that MET-PET might provide clinically useful and reliable information about the pathology underlying epileptogenic brain tumours.

Some methodological issues must be discussed. Firstly, changes in imaging procedures occurred during the course of this study, resulting in two different PET acquisition protocols, and lack of 3D MRI data in a minority of patients. However, these changes are unlikely to have biased our results, since the proportion of each tumour type was comparable in all the resulting subgroups. Most previous MET-PET studies used circular or irregular ROIs traced around the tumours in comparison with contralateral homotopic or cortical regions, but it is noteworthy that the exact type of ROI has varied from one series to another.[22 26–29 31 32 34] We used the different types of ROI and index most commonly reported in other studies to ensure that our results were not dependent on a specific method of PET data analysis. In fact, most of the differences observed between the various types of tumour were demonstrated with all the three parameters employed in this study.

Secondly, visual analysis was performed blinded to all other data except the anatomical location of the tumour to address the issue most relevant to clinical practice—that is, the PET findings within the tumour. Regardless of the limitations and subjectivity of visual analysis, it must be acknowledged that the clinical use of PET imaging partly relies on the possibility of obtaining reliable visual interpretation of the data in daily practice. The criteria proposed in the present study to detect and classify abnormal tumour methionine uptake appear appropriate for such clinical application; they proved easy to use and reliable, allowing for fully consensual reports of two independent investigators and providing results consistent with semiquantitative data.

Table 3 Correlation* between qualitative MET-PET data and pathology (n = 27)

	Pathological data (n (%))		
Visual methionine uptake	Dysembryoplastic neuroepithelial tumours	Gangliogliomas	Gliomas
Normal	7 (63)	0	0
Moderate increase	4 (37)	4 (80)	3 (27)
Marked increase	0	1 (20)	8 (73)
Total	11	5	11

*p<0.0002.

Lastly, regarding the reliability of our patients' pathological diagnosis, several authors have emphasised the difficulty in establishing the neuropathological diagnosis of DNT.[4 9] The diagnosis is partly based on the presence of the ''glioneuronal element'', a specific figure which could be missing in non-specific forms of DNT,[9 40] or when the tumour has been removed incompletely. In our series, all patients underwent complete removal of their tumour except for three patients, whose biopsy specimens provided sufficient information to ensure a definite diagnosis. In addition, as described in the Methods section our selection criteria included a reliable pathological diagnosis made by pathologists trained to in the evaluation of glioneuronal tumours, including experts from other institutions when necessary.

One of our main findings was that only DNTs, and more specifically mesial temporal DNTs, were associated with a normal tumour methionine uptake, suggesting that this pattern could be specific of this tumour type, at least in the context of a non-rapidly progressing brain mass lesion associated with an epilepsy of more than six months' duration. Similar findings were recently reported in a small series of seven epileptogenic tumours, including four DNTs, one ganglioglioma, and two low grade gliomas.[39] In contrast, several authors have reported the possibility of normal MET-PET findings in low grade astrocytomas.[22–24 27 29 34 41] Some of these studies were conducted before DNT was clearly recognised, suggesting the possibility that some of these astrocytomas were DNTs.[22–24 29] In other, more recent, studies[27 34] pathological examination of up to half of the specimens was based on a biopsy again raised the possibility of misdiagnosed DNT.[8] Thus none of the series that have reported normal MET-PET findings in low grade gliomas included DNTs, despite the fact that the latter represents up

Table 4 Correlation between semiquantitative [^{11}C]-methionine positron emission tomography and pathological data

	Mean (SD) T/C (n = 20)	Max (SD) T/C (n = 25)	OR (SD) (n = 25)
Dysembryoplastic neuroepithelial tumours	1.03 (0.2) (n = 8)	1.37 (0.4) (n = 9)	0.91 (0.3) (n = 9)
Gangliogliomas	1.58 (0.3) (n = 4)	2.06 (0.3) (n = 5)	1.12 (0.2) (n = 5)
Low grade gliomas	1.77 (0.3) (n = 6)	2.56 (0.7) (n = 7)	1.68 (0.57) (n = 7)
High grade gliomas	1.48 (0.4) (n = 2)	3.87 (1.3) (n = 4)	2.02 (0.47) (n = 4)

Max T/C, maximal tumour-to-contralateral homotopic ratio; Mean T/C, Mean tumour-to-contralateral homotopic ratio; OR, tumour-to-contralateral occipital ratio.

to 65% of brain neoplasms responsible for chronic drug resistant epilepsy.[4] Apart from the issue of misdiagnosed DNTs, discrepancies between our results and former series might reflect differences in the rates of chronic drug resistant partial epilepsy in the population studied. In that respect, it is important to stress that the common forms of low grade astrocytomas are rarely encountered in patients with tumour associated chronic epilepsy, and were not observed even in a recent series of 94 epilepsy surgery tumour cases.[4] Finally, some authors have proposed that protoplasmic astrocytomas in cortical locations associated with chronic epilepsy correspond to non-specific forms of DNT.[9] Overall, whether the lack of a visually detectable increased methionine uptake is specific to DNTs, or that it may also occur with other epileptogenic tumours, remains an open issue that needs to be addressed in a larger population.

Semiquantitative analysis of the DNT cases presented in this study resulted in an average max T/C ratio for DNTs within a previously reported range for low grade gliomas.[41] It must be noted, however, that there was a significant difference between DNTs with and without visually detectable increased methionine uptake (average max T/C 1.76 and 1.07, respectively; $p<0.05$). With regard to the other tumour types, our results are generally in agreement with those of previously published studies. All oligodendrogliomas, as well as all high grade gliomas were associated with an abnormal increased methionine uptake, as has been reported by others.[26 27 31 34] In contrast, gangliogliomas stood apart from gliomas, in that they were only rarely associated with a marked MET-PET abnormality (20%). However, the small number of cases included in this study tempers this finding. We found a single report of a MET-PET study[39] in a patient with a temporal ganglioglioma, which was consistent with our own findings, as well as another report of a patient investigated with single photon emission computed tomography (SPECT) that demonstrated an increased methyltyrosine uptake.[42] According to the various ratios that we calculated, gangliogliomas appear to be associated with an average degree of increased methionine uptake intermediate between that of DNTs and gliomas. This is consistent with the risk of malignant transformation of these tumours, estimated around 10%, a low figure compared with that for gliomas but still higher than that for DNTs (which is virtually nil).[10]

Our findings raise several pathophysiological issues. A prevailing hypothesis is that the increased methionine uptake observed in tumoral cells reflects an upregulation of the amino acid transport system[43–47] caused by increased protein metabolism and cellular proliferation.[45 48] Our results regarding gangliogliomas and DNTs are consistent with this hypothesis, since most of these two types of well differentiated glioneuronal tumour are characterised by a lower proliferative index[9–11 49–52] and methionine uptake than gliomas. Conversely, it has been suggested that the breakdown of the blood–brain barrier, as partly reflected by the presence of gadolinium enhancement on MRI, significantly contributes to MET-PET abnormalities.[53] Thanks to the peculiarities of epileptogenic glioneuronal tumours, where gadolinium enhancement proved to be as frequent as in gliomas in this study, it seems unlikely that the breakdown of the blood–brain barrier had played a significant role in our results. Indeed, all DNTs with gadolinium enhancement had normal MET-PET findings, whereas all DNTs with abnormal MET-PET findings lacked gadolinium enhancement.

From a clinical point of view, the preoperative distinction of DNT from other epileptogenic tumours may have several important consequences. Firstly, it could assist the pathologist in difficult to diagnose DNT cases where the specific glioneuronal element is missing. Secondly, it could help deciding whether surgical removal of the suspected tumour is indicated. For instance, in a patient whose epilepsy is well controlled by antiepileptic drugs and surgical treatment is not justified per se, one could balance the risk of removing a DNT, in particular when located in the dominant mesiotemporal structures, with that of its natural long term evolution. As a rule this is benign, with a single published case of suspected malignant transformation.[14] According to the present study, normal methionine uptake within a mesial temporal epileptogenic tumour is suggestive of an underlying DNT, whereas the presence of markedly increased methionine uptake makes the diagnosis of either DNT or ganglioglioma unlikely.

ACKNOWLEDGEMENTS

We wish to thank S Bouvard, I Merlet, and C Pierre from the CERMEP for their helpful advice and comments, as well as Professors C Daumas-Duport, Saint-Anne Hospital, and B Pasquier, Albert Michallon Hospital, France, for reviewing some of the pathological specimens.

Authors' affiliations

D S Rosenberg, G Demarquay, F Mauguière, P Ryvlin, Department of Functional Neurology and Epileptology, Hopital Neurologique, Lyon, France
A Jouvet, N Streichenberger, N Kopp, Department of Neuropathology, Hopital Neurologique, Lyon, France
D Le Bars, P Ryvlin, CERMEP, Hopital Neurologique, Lyon, France
M Sindou, Department of Neurosurgery, Hopital Neurologique, Lyon, France

Competing interests: none declared

This study was approved by the CCPPRB local ethic committee (Comité Consultatif de Protection des Personnes se prêtant à des Recherches Biomédicales—Centre Léon Bérard, Lyon)

REFERENCES

1 **Wolf HK**, Wiestler OD. Surgical pathology of chronic epileptic seizure disorders. *Brain Pathol* 1993;**3**:371–80.
2 **Plate KH**, Wieser HG, Yasargil MG, *et al*. Neuropathological findings in 224 patients with temporal lobe epilepsy. *Acta Neuropathol* 1993;**86**:433–8.
3 **Pasquier B**, Bost F, Peoc'h M, *et al*. Neuropathological findings in resective surgery for medically intractable epilepsy. *Ann Pathol* 1996;**16**:174–81.
4 **Pasquier B**, Péoc'h M, Fabre-Bocquentin B, *et al*. Surgical pathology of drug-resistant partial epilepsy. A 10-year-experience with a series of 327 consecutives resections. *Epileptic Disord* 2002;**4**:99–119.
5 **Fried I**, Kim JH, Spencer DD. Limbic and neocortical gliomas associated with intractable seizure: a distinct clinicopathological group. *Neurosurgery* 1994;**34**:815–24.
6 **Bartolomei JC**, Christopher S, Vives K, *et al*. Low-grade gliomas of chronic epilepsy: a distinct clinical and pathological entity. *J Neurooncol* 1997;**34**:79–84.
7 **Honavar M**, Janota I, Polkey CE. Histological heterogeneity of dysembryoplastic neuroepithelial tumor: identification and differential diagnosis in a series of 74 cases. *Histopathology* 1999;**34**:342–56.
8 **Daumas-Duport C**, Scheitauer BW, Chodkiewicz, et al. Dysembryoplastic neuroepithelial tumor: a surgical curable tumor of young patients with intractable partial seizures. Report of 39 cases. *Neurosurgery* 1988;**23**:545–56.
9 **Daumas-Duport C**. Dysembryoplastic neuroepithelial tumours. *Brain Pathol* 1993;**3**:283–95.
10 **Kleihues P**, Cavenee WK. *Pathology and Genetic Tumours of the Nervous System*. Lyon: IARC Press, 2000.
11 **Miller DC**, Lang FF, Epstein FJ. Central nervous system gangliogliomas. Part 1: Pathology. *J Neurosurg* 1993;**79**:859–66.
12 **Rumana CS**, Valadka AB. Radiation therapy and malignant degeneration of benign supratentorial gangliogliomas, *Neurosurgery* 1998;**42**:1038–43.
13 **Rushing EJ**, Thompson LD, Mena H. Malignant transformation of a dysembryoplastic neuroepithelial tumor after radiation and chemotherapy. *Ann Diagn Pathol* 2003;**7**:240–4.
14 **Hammond RR**, Duggal N, Woulfe JMJ, *et al*. Malignant transformation of a dysembryoplastic neuroepithelial tumor. Case report. *J Neurosurg* 2000;**92**:722–5.
15 **Stanescu Cosson R**, Varlet P, Beuvon F, *et al*. Dysembryoplastic neuroepithelial tumors: CT, MR findings and imaging follow-up: a study of 53 cases. *J Neuroradiol* 2001;**28**:230–40.
16 **Di Chiro G**, De La Paz RL, Brooks RA, *et al*. Glucose utilization of cerebral gliomas measured by 18 fluorodeoxyglucose and positron emission tomography. *Neurology* 1982;**32**:1323–9.

17 **Di Chiro G**. Positron emission tomography using [^{18}F] fluorodeoxyglucose in brain tumors: A powerful diagnostic and prognostic tool. *Invest Radiol* 1986;**22**:360–71.
18 **Di Chiro G**, Brooks RA. PET-FDG of untreated and treated cerebral gliomas. *J Nucl Med* 1988;**29**:421–2.
19 **Coleman RE**, Hoffman JM, Hanson MW, *et al*. Clinical application of PET for the evaluation of brain tumors. *J Nucl Med* 1991;**32**:616–22.
20 **Kim CK**, Alavi JB, Alavi A, *et al*. New grading system of cerebral gliomas using positron emission tomography with ^{18}F-fluorodeoxyglucose. *J Neurooncol* 1991;**10**:85–91.
21 **Roelcke U**. PET: brain tumor biochemistry. *J Neurooncol* 1994;**22**:275–9.
22 **Ericson K**, Lilja A, Bergström M, *et al*. PET with ^{11}C-methyl-L-methionine, ^{11}C-D-glucose and ^{68}Ga-EDTA in supratentorial tumors. *J Comput Assist Tomogr* 1985;**9**:683–9.
23 **Lilja A**, Bergström K, Hartvig P, *et al*. Dynamic study of supratentorial gliomas with L-methyl -^{11}C methionine and PET. *AJNR Am J Neuroradiol* 1985;**6**:505–14.
24 **Bustany P**, Chatel M, Derlon JM, *et al*. Brain tumor protein synthesis and biological grades: a study by PET with ^{11}C-L-Methionine. *J Neurooncol* 1986;**3**:397–404.
25 **Mineura K**, Sasajima T, Kowada M, *et al*. Innovative approach in the diagnosis of gliomatosis cerebri using Carbon-11-L-Methionine PET. *J Nucl Med* 1991;**32**:726–8.
26 **Derlon JM**, Bourdet C, Bustany P, *et al*. ^{11}C-L-Methionine uptake in gliomas. *Neurosurgery* 1989;**25**:720–8.
27 **Derlon JM**, Petit-Taboué MC, Chapon F, *et al*. The in vivo metabolic pattern of low-grade brain gliomas: a PET study using ^{18}FDG and ^{11}C-L-methionine. *Neurosurgery* 1997;**40**:276–88.
28 **Derlon JM**, Chapon F, Noël MH, *et al*. Non-invasive grading of oligodendrogliomas: correlations between in vivo metabolic pattern and histopathology. *Eur J Nucl Med* 2000;**27**:778–7.
29 **Ogawa T**, Shishido F, Kanno I, *et al*. Cerebral gliomas: evaluation with methionine PET. *Radiology* 1993;**186**:45–53.
30 **Ogawa T**, Inugami A, Hatazawa J, *et al*. Clinical PET for brain tumors: comparison of ^{18}FDG and L-methyl-^{11}C-methionine. *AJNR Am J Neuroradiol* 1996;**17**:345–53.
31 **Herholz K**, Hölzer T, Bauer B, *et al*. ^{11}C-Methionine PET for differential diagnosis of low-grade gliomas. *Neurology* 1998;**50**:1316–22.
32 **Kaschten B**, Stevenaert A, Sadzot B, *et al*. Preoperative evaluation of 54 gliomas by PET with Fluorine-18-fluorodeoxyglucose and/or carbon-11-methionine. *J Nucl Med* 1998;**39**:778–85.
33 **Roelcke U**, Radü EW, Hausmann O, *et al*. Tracer transport and metabolism in a patient with juvenile pilocytic astrocytoma. A PET study. *J Neurooncol* 1998;**36**:279–83.
34 **De Witte O**, Goldberg I, Wikler D, *et al*. PET with injection of methionine as a prognostic factor in glioma. *J Neurosurg* 2001;**95**:746–50.
35 **Provenzale JM**, Arata MA, Turkington TG, *et al*. Gangliogliomas: characterization by registered PET-MR images. *AJR Am J Roentgenol* 1999;**172**:1103–7.
36 **Kincaid P**, El-Saden S, Park SH, *et al*. Cerebral gangliogliomas: preoperative grading using FDG-PET and ^{201}Tl-SPECT. *AJNR Am J Neuroradiol* 1998;**19**:801–6.
37 **Meyer PT**, Spetzger U, Mueller H, *et al*. High F18-FDG uptake in a low-grade supratentorial gliomas: a PET case report. *Clin Nucl Med* 2000;**25**:694–7.
38 **Kaplan AM**, Lawson MA, Sparato J, *et al*. PET using ^{18}FDG and ^{11}C-L-methionine to metabolically characterise dysembryoplastic neuroepithelial tumors. *J Child Neurol* 1999;**14**:673–7.
39 **Maehara T**, Nariai T, Arai N, *et al*. Usefulness of ^{11}C-Methionine PET in the diagnosis of dysembryoplastic neuroepithelial tumor with temporal lobe epilepsy. *Epilepsia* 2004;**45**:41–5.
40 **Varlet P**, Beuvon F, Fallet-Bianco C, *et al*. Dysembryoplastic neuroepithelial tumors. *Ann Pathol* 2000;**20**:429–37.
41 **Kracht LW**, Friese M, Herholz K, *et al*. Methyl-[11C]-L-methionine uptake as measured by positron emission tomography correlates to microvessel density in patients with glioma. *Eur J Nucl Med Mol Imaging* 2003;**30**:868–73.
42 **Woesler B**, Kuwert T, Kulermann G. High amino-acid uptake in a low-grade desmoplastic infantile ganglioglioma in a 14-year-old patient. *Neurosurg Rev* 1998;**21**:31–5.
43 **Langen KJ**, Ziemons K, Kiwit J, *et al*. 3-^{123}I-Iodo-Methyl-tyrosine and Methyl-^{11}C-L-methionine uptake in cerebral gliomas: a comparative study using PET and SPECT. *J Nucl Med* 1997;**38**:517–22.
44 **Johnstone RM**, Scholefield PG. Amino-acid transport in tumor cells. In: Haddow A, Weinhouse S, eds. *Advances in Cancer Research*. Edinburgh: Academic Press, 1965:9.
45 **Langen KJ**, Mühlensiepen H, Holschbach M, *et al*. Transport mechanisms of 3-^{123}Iodo-methyl-L-tyrosine in a human glioma cell line: comparison with ^{3}H-methyl-L-methionine. *J Nucl Med* 2000;**41**:1250–5.
46 **Bergström M**, Ericson K, Hagenfeldt L, *et al*. PET study of methionine accumulation in glioma and normal brain tissue: competition with branched chain amino acids. *J Comput Assist Tomogr* 1987;**11**:208–13.
47 **Ishiwata K**, Kubota K, Murakami M, *et al*. M. Re-evaluation of amino acid PET studies: can the protein synthesis rates in brain and tumor tissues be measured in vivo. *J Nucl Med* 1993;**34**:1936–43.
48 **Sato N**, Suzuki M, Kuwata N, *et al*. Evaluation of the malignancy of glioma using 11-C-methionine positron emission tomography and proliferating cell nuclear antigen staining. *Neurosurg Rev* 1999;**22**:210–14.
49 **Wolf HK**, Müller MB, Spänle M, *et al*. Ganglioglioma: a detailed histopathological and immunohistochemical analysis of 61 cases. *Acta Neuropathol* 1994;**88**:166–73.
50 **Prayson RA**, Khajavi K, Comair YG. Cortical architectural abnormalities and MIB1 immunoreactivity in gangliogliomas: a study of 60 patients with intracranial tumors. *J Neuropathol Exp Neurol* 1995;**54**:513–20.
51 **Prayson RA**, Morris HH, Estes ML, *et al*. Dysembryoplastic neuroepithelial tumor: a clinical an immunohistochemical study of 11 tumors including MIB1 immunoreactivity. *Clin Neuropathol* 1996;**15**:47–53.
52 **Raymond AA**, Halpin SF, Alsanjari N, *et al*. Dysembryoplastic neuroepithelial tumour. Features in 16 patients. *Brain* 1994;**117**:461–75.
53 **Roelcke U**, Radü EW, von Ammon K, *et al*. Alteration of blood-brain barrier in human brain tumors: comparison of ^{18}FDG, ^{11}C-methionine and rubidium-82 using PET. *J Neurol Sci* 1995;**132**:20–7.